

HIV-Reverse Transcriptase Inhibition: Inclusion of Ligand-Induced Fit by Cross-Docking Studies

Rino Ragno,^{*,†} Simona Frasca,[†] Fabrizio Manetti,[‡] Antonella Brizzi,[‡] and Silvio Massa^{*,‡}

Dipartimento di Studi di Chimica e Tecnologie delle Sostanze Biologicamente Attive, Università di Roma "La Sapienza", piazzale Aldo Moro 5, I-00185 Roma, Italy, and Dipartimento Farmaco Chimico Tecnologico, Università degli Studi di Siena, via A. Moro, I-53100 Siena, Italy

Received July 29, 2004

Nonnucleoside reverse transcriptase inhibitors (NNRTIs) have, in addition to the nucleoside reverse transcriptase inhibitors (NRTIs) and protease inhibitors (PIs), a definitive role in the treatment of HIV-1 infections. Since the appearance of HEPT and TIBO, more than 30 structurally different classes of compounds have been reported as NNRTIs, which are specific inhibitors of HIV-1 replication, targeting the HIV-1 reverse transcriptase (RT). Nevirapine and delavirdine are the first formally licensed for clinical use, and others have been licensed afterward, while several are in preclinical or clinical development. The NNRTIs interact with a specific site of HIV-1 RT (nonnucleoside binding site, NNBS) that is close to, but distinct from, the NRTI binding site. In this work we report the application of the Autodock program assessing its usability through reproduction of 41 NNRTI experimental bound conformations. Moreover, cross-docking experiments on the wild-type and mutated RT forms were conducted to take into account the enzyme flexibility as a valuable tool for structure-based drug design (SBDD) studies and to gain insight on the mode of action of new anti-HIV agents active against both wild-type and resistant strains.

Introduction

Failure of HIV monotherapy,¹ due to the growth of resistant viral variants, moved attention to a therapy that uses a combination of potent antiviral agents. This treatment is called HAART, highly active antiretroviral therapy.²

Nonnucleoside reverse transcriptase inhibitors (NNRTIs) such as zidovudine³ (TIBO derivative) and zalcitabine³ (an alpha-APA derivative) were the first to have a significant activity against wild-type enzyme of HIV-1, but they had no effect against mutants.

This led to the study of chemical and structural modifications of these compounds for designing new NNRTIs effective against a wide range of mutants.^{4,5}

Crystal structure analysis of HIV-RT enzyme showed that the first generation of drugs (TIBO, alpha-APA, Nevirapine) filled up an allosteric hydrophobic pocket (nonnucleoside binding site, NNBS) and bound the enzyme in a "butterfly-like" mode.⁶ One of the "wings" of this butterfly is made of π -electron-rich moiety (phenyl or allyl substituents) that interacts through π - π interactions with a hydrophobic pocket formed mainly by the side chains of aromatic amino acids (Tyr181, Tyr188, Phe227, Trp229, and Tyr318). On the other hand, the other wing is normally represented by a heteroaromatic ring bearing on one side a functional group capable of donating and/or accepting hydrogen bonds with the main chain of the Lys101 and Lys103. Finally, on the butterfly body a hydrophobic portion

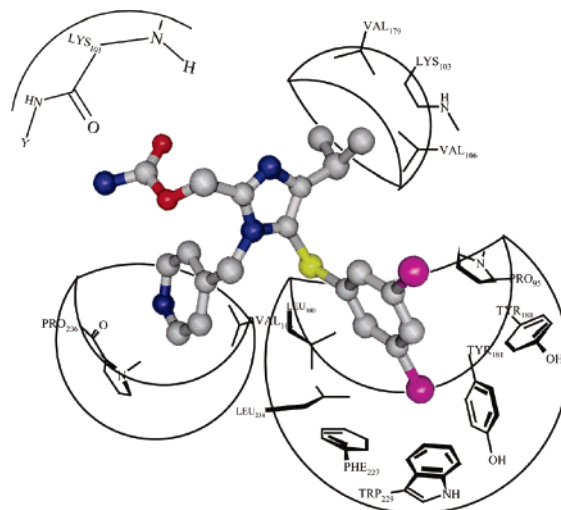


Figure 1. Schematic view of the NNBS. The experimentally bound conformation of the ligand in the 1EP4 complex is also reported.

fulfills a small pocket formed mainly by the side chains of Lys103, Val106, and Val179 (Figure 1).

Upon complexation the NNBS hydrophobic pocket changes its own conformation leading to inactivation of the enzyme itself. Because of the different chemical and structural features of the inhibitors and the side-chain flexibility, the bound NNBS undergoes different conformations.⁷ Moreover, mutations of some amino acids cause a variation of the NNBS pocket properties, thus decreasing affinities of most the inhibitors.⁸

In particular, the NNRTI resistance mutation of Tyr188 and Tyr181 reduces π - π interactions; the G190A mutation leads to a lower active-site space because of a steric conflict between the methyl side

* To whom correspondence should be addressed. R.R.: phone, +39 6 4991 3152; fax, +39 6 491 491; e-mail, rino.ragno@uniroma1.it. S.M.: phone, +39 577 234332; fax, +39 577 234333; e-mail, massa@unisi.it.

[†] Università degli Studi di Siena.

[‡] Università degli Studi di Roma "La Sapienza".

Table 1. PDB Code, Ligand Name, Ligand Structures, and Residue Mutations of the 41 RT Complexes Used in the Present Study

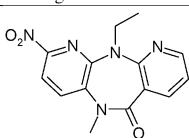
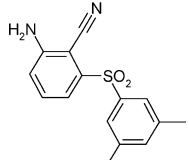
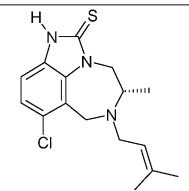
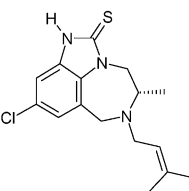
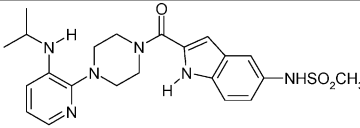
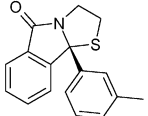
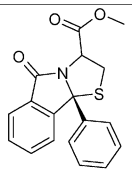
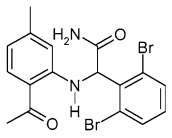
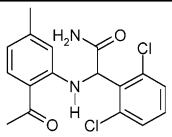
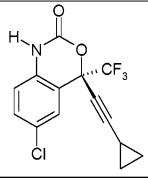
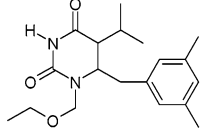
PDB Code	Ligand Name	Ligand structure	Mutation(s)	Ref.
IRT3	1051U91		D67N, K70R, T215F, K219Q	32
1RTH			None	33
1JLQ	739W94		None	34
1HNV	8-Cl TIBO R86183		C280S	35
1UWB			Y181C, C280S	36
1REV	9-Cl TIBO R82913		None	37
1TVR			C280S	36
1KLM	BHAP U-90152 Delarvidine		None	38
1COT	BM+21.1326		None	39
1COU	BM+50.0934		None	39
1HNI	Br2 α-APA R95845		C280S	40
1VRU	Cl2 α-APA R90385		None	41
1FK9	Efavirenz		None	42
1FKO			42	
1IKV			K103N	43
1IKW			44	
1JKH			Y181C	45
1C1B	GCA-186		None	46

Table 1 (Continued)

1BQM			C280S	47
	HBY 097			
1BQN			Y188L, C280S	47
1RTI	HEPT		None	33
1RT1	MKC-442		None	48
1IKY	MSC194		K103N	44
1EET	MSC204		None	49
1FKP			K103N	42
1JLB	Nevirapine		Y181C	45
1JLF			Y188C	45
1VRT			None	33
1DTT	PETT130A94 (PETT-2)		None	50
1JLC			Y181C	45
1DTQ	PETT131A94 (PETT-1)		None	50
1IKX	PNU142721		K103N	44
1EP4	S-1153		None	51
1C1C	TNK-6123		None	46
1JLA	TNK-651		Y181C	45
1RT2			None	48

Table 1 (Continued)

IRT5	UC-10		None	52
IRT6	UC-38		None	52
IJLG	UC-781		Y188C	45
IRT4			None	52
IRT7	UC-84		None	52

chain and the inhibitor, and the formation of a hydrogen bond between K103N and Tyr188 reduces the inhibitor entering in the NNBS.⁹

In view of the above observations, the design of new NNRTIs must consider structures with high conformational freedom to suit the different steric conformations of NNBS and, at the same time, must contain suitable chemical features capable of interact with highly conserved residues such as Trp229 (part of the “primer grip”).¹⁰

X-ray crystal structures of ligand–protein cocomplexes have been important tools for medicinal chemists in the discovery, design, and optimization of drug candidates.^{11–13} These structural data, along with the computational analysis tools that have been developed to implement structure-based drug design (SBDD), have proved to be very successful in medicinal chemistry. As a greater number of X-ray crystal structures become available to medicinal chemists, with the advent of structural genomics,¹⁴ computational methods that take advantage of protein–ligand structural data are becoming more critical to the drug design process.

Several docking programs are now available. Among them, many are able to consider the flexibility of the ligand while maintaining the protein rigid.^{15–22} We focused on application of the Autodock²² program which has been widely used with success in reproducing the bound conformation of different ligand/protein systems.²³ Although some limited docking and cross-docking studies have been reported on the RT system using other programs,^{24–28} to date, except for some single applications,^{29–31} no extensive use of the Autodock program has been reported in the case of reverse transcriptase inhibitors.

In this paper we report the application of Autodock to 41 NNRTI cocrystallized with the RT (Table 1). This docking study was twofold: first, each ligand was docked in the native protein in order to assess the reliability of the docking program and, second, an extensive cross-docking of every ligand in each non-native RT enzyme was conducted to inspect the ligand adaptability to different states of the experimentally determined bound NNBS. Moreover, the cross-docking experiment was also conducted on the mutated forms of RT to see if it would be of some help to discriminate between active and nonactive compounds against mutated RTs.

Table 2. Assessment of the Autodock Program. RMSD Values for the First Ranked Pose, the Lowest Energy Docked Conformation of the Most Populated Cluster, and the One Closest to the Experimentally Bound Conformation Are Reported^a

PDB	best docked		best cluster		lowest RMSD	
	cluster	RMSD	cluster	RMSD	cluster	RMSD
1BQM	1	1.53	1	1.53	4	0.84
1BQN	1	1.18	2	1.45	1	1.07
1C0T	1	2.38	3	0.86	3	0.59
1C0U	1	2.35	2	0.86	2	0.69
1C1B	1	0.82	1	0.82	1	0.59
1C1C	1	1.16	1	1.16	1	0.69
1DTQ	1	1.44	1	2.23	2	0.58
1DTT	1	1.49	2	0.85	2	0.84
1EET	1	1.06	1	1.06	1	1.07
1EP4	1	0.89	1	0.89	1	0.89
1FK0	1	0.41	1	0.41	1	0.36
1FK9	1	0.35	1	0.35	1	0.24
1FKP	1	1.06	1	1.06	1	1.04
1HNI	1	0.61	1	0.61	1	0.43
1HNV	1	1.20	1	1.20	1	0.97
1IKV	1	0.33	1	0.33	1	0.25
1IKW	1	0.30	1	0.30	1	0.11
1IKX	1	0.89	1	0.89	1	0.64
1IKY	1	1.15	1	1.15	1	0.83
1JKH	1	0.86	1	0.86	1	0.56
1JLA	1	1.03	1	1.03	1	0.98
1JLB	1	1.41	1	1.41	1	0.59
1JLC	1	1.77	2	1.36	2	0.87
1JLF	1	1.24	1	1.24	1	1.16
1JLG	1	1.26	1	1.26	1	1.00
1JLQ	1	0.90	1	0.90	1	0.48
1KLM	1	1.42	1	1.42	1	1.03
1REV	1	1.00	1	1.00	1	0.75
1RT1	1	0.90	1	0.90	1	0.76
1RT2	1	0.99	1	0.99	1	0.71
1RT3	1	0.83	1	0.83	1	0.81
1RT4	1	1.16	1	1.16	1	1.08
1RT5	1	0.81	1	0.81	1	0.76
1RT6	1	1.57	1	1.57	1	1.30
1RT7	1	1.30	1	1.30	1	1.22
1RTH	1	1.16	1	1.16	1	1.08
1RTI	1	1.51	1	1.51	1	1.04
1TVR	1	3.05	2	0.63	2	0.61
1UWB	1	0.61	1	0.61	1	0.60
1VRT	1	3.00	3	1.54	3	1.12
1VRU	1	2.07	2	0.70	2	0.63

^a RMSD values are referred to IVRT.

Results and Discussion

Assessment of Docking. Although almost 50 ligand/RT complexes are available, no extensive use of any molecular docking program has yet been reported on

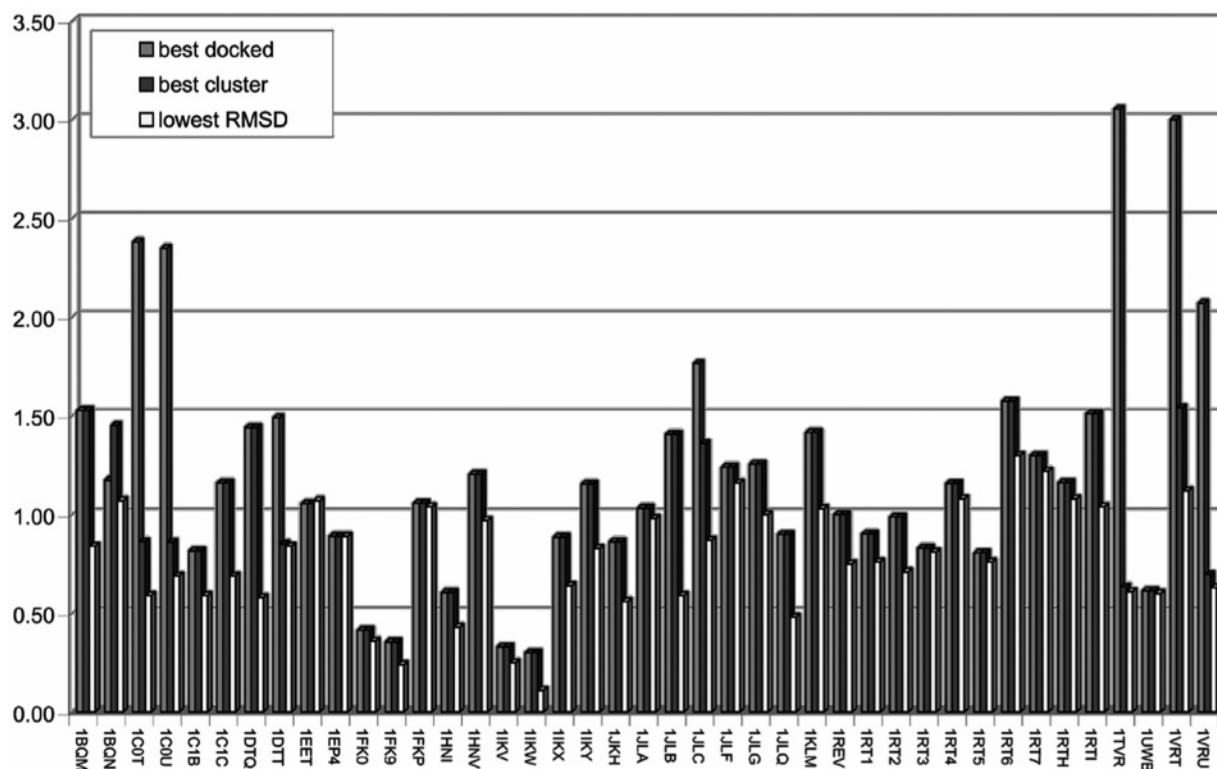


Figure 2. Assessment of the Autodock program. Graphical comparison of the RMSD values obtained for the first ranked pose, the lowest energy docked conformation of the most populated cluster, and the one closest to the experimentally bound conformation

this important issue (while this manuscript was in preparation a cross-docking experiment on 18 HIV-RT was reported by Daeyaert et al.²⁷ using an in-house pharmacophore docking algorithm). Thus far, only limited docking and cross-docking experiments on the RT system have been previously reported: Titmuss et al.²⁴ applied the DOCK program to a limited set of seven RT complexes reporting that a uniform ligand binding mode can occur, although they experimentally observed flexibility of the NNBS; Halgren et al.²⁵ used the 1VRT and 1RT1 complexes as RT complex examples to evaluate the docking accuracy of the docking program GLIDE; Wang et al.⁵³ and Ranise et al.²⁸ applied the DOCK 4.0 program to dock the PETT-1 (1DTQ) and 8CI-TIBO (1UWB), respectively; Zhou et al.²⁶ used the 1VRT and 1RTH to validate the MOE-dock program and study the binding mode of several diterpenoids as NNRTI; Autodock 3.0 was recently used for structure-based drug design studies on new DABO,²⁹ APAS,³⁰ arylthiopyridylmethylisopropylpyrrole carbinols,³¹ and small peptide RT inhibitors⁵⁴ assessing the usability of the program by reproducing the bound conformations of MKC-442 (1RT1), 739W94 (1JLQ), S-1153 (1EP4), and UC-781 (1RT4), respectively. To assess the usability of the nonprofit free Autodock program, we performed docking studies on 41 RT complexes (see Table 1, Materials and Methods). Although it has been reported that for a high-throughput screening only the first-ranked docked conformation (hereafter referred to as the best docked conformation) should be considered,²⁰ we are confident that in the case of the Autodock program in some cases the lowest energy docked conformation of the most populated cluster (herein named best cluster conformation) should be also taken into account.⁵⁵ In Table 2 and Figure 2 the RMSD for the

best docked, best cluster, and lowest RMSD values found are reported. It is clear that in those cases where the best cluster conformation does not coincide with the best docked conformation (1BQN, 1C0T, 1C0U, 1DTT, 1JLC, 1TVR, 1VRT, and 1VRU), a better RMSD value is observed except for 1BQN (whose values were although quite similar) increasing from 87.8% (best docked) to 100% (lowest RMSD) the percentage of the number of conformations found below the threshold value of 2.0 Å. Indeed, if one considered all the docked conformations, the accuracy of the docking would be even better, obtaining 70.7% of conformations docked with RMSD values below 1 Å, while for the best cluster and best docked only 48.8% and 36.6% of RMSD values, respectively, were found under a very restrictive threshold of 1 Å. These good values assess the usability of the Autodock program for the RT system.

Cross-Docking. Wild-Type RTs. In the previous section we demonstrated the ability of the Autodock program in reproducing the binding mode of several known bound conformations of NNRTI. A striking feature of RT is its considerable conformational flexibility^{56,57} (believed to be essential for several of its catalytic actions),⁵⁸ which has complicated attempts at traditional structure-based drug design (SBDD) of non-nucleoside RT inhibitors (NNRTIs).⁵⁹

As a measure of the RT flexibility, the RMSD values (using the 1VRT complex as a reference) for the 182 selected RT residues (see Materials and Methods) and for each residue in a 5 Å core of the NNBS (Pro95A, Leu100A-Lys103A, Val106A, Tyr115A, Val179A-Tyr181A, Tyr188A-Gly190A, Lys219A, Thr215A, Phe227A, Trp229A, Leu234A-Pro236A, Tyr318A) have been calculated and reported in Table 3. For the backbone atoms (C, O, CA, and N in the PDB notation) the RMSD value

Table 3. Flexibility of Wild-type RTs^a

PDB code	20 Å core										residues in 5 Å core																
	all atoms					backbone					Pro95	Leu100	Lys101	Lys102	Lys103	Val106	Val179	Ile180	Tyr181	Tyr188	Val189	Gly190	Phe227	Trp229	Leu234	His235	Pro236
Ibqm	1.71	1.24	0.77	0.38	1.73	2.59	2.31	0.97	0.95	0.63	0.66	0.80	0.39	0.39	0.52	0.56	2.31	1.49	1.69	1.56	0.63						
Ic0t	1.09	0.57	0.34	0.36	0.43	1.43	0.49	0.53	0.64	0.63	1.44	0.39	0.29	0.37	0.98	0.98	0.39	0.65	0.42	0.59	0.47						
Ic0u	1.86	1.38	0.83	0.53	1.09	2.11	0.90	0.84	0.86	0.49	1.38	0.52	0.65	0.66	0.96	0.96	2.80	1.36	1.08	1.01	0.67						
Ic1b	1.94	1.55	0.23	0.44	1.47	1.33	0.62	1.06	0.63	0.47	1.47	0.97	0.97	0.80	0.85	0.85	0.88	0.71	1.54	2.27	0.79						
Ic1c	1.97	1.47	0.63	0.63	1.65	1.19	0.80	0.88	1.00	0.42	1.41	0.69	0.88	0.76	1.11	1.11	2.76	1.36	1.36	2.20	0.87						
Ic1q	1.21	0.64	0.50	0.31	1.11	1.08	0.64	0.42	0.51	0.36	1.44	1.00	0.50	0.52	0.78	0.78	1.16	1.51	1.44	0.75	0.49						
Ic1t	1.65	1.14	0.50	0.44	1.11	1.37	0.43	0.44	0.37	0.39	1.44	0.59	0.27	0.22	0.79	0.79	2.93	1.44	1.48	0.96	0.60						
Ic2t	1.62	0.90	0.26	0.27	0.79	0.74	0.79	1.54	0.31	0.27	0.19	0.56	0.33	0.29	0.82	0.82	0.86	1.39	1.09	1.71	1.45						
Iep4	2.57	2.22	1.82	0.85	1.90	1.67	1.34	1.87	0.82	0.40	1.83	1.78	1.23	1.07	0.71	0.71	1.18	0.89	2.44	3.15	1.45						
Iff*9	0.95	0.48	0.45	0.41	0.66	0.80	0.44	1.47	0.53	0.42	1.48	1.47	0.32	0.19	0.34	1.06	0.58	1.31	0.31	0.28	0.36						
Ihni	1.75	1.28	1.30	0.32	1.81	0.76	0.75	0.82	0.81	0.37	0.29	0.64	0.60	0.33	1.06	1.06	1.01	1.48	1.32	0.94	0.27						
Ihmv	1.66	1.11	0.50	0.30	1.03	1.09	0.85	0.98	0.66	0.54	1.42	0.64	0.49	0.27	1.04	1.04	2.68	1.10	1.02	1.06	0.64						
Ij1q	1.58	1.13	0.59	0.30	1.03	1.09	0.85	0.98	0.66	0.54	1.42	0.64	0.49	0.27	1.04	1.04	2.68	1.10	1.02	1.06	0.64						
Iklm	1.99	1.53	0.45	0.62	1.75	0.89	1.38	1.54	0.91	0.68	0.57	0.76	1.00	0.97	1.49	1.49	1.56	2.09	2.01	3.55	1.04						
Irev	1.32	0.62	0.45	0.51	0.79	1.02	0.81	0.55	1.33	0.34	0.42	0.62	0.55	0.41	0.74	0.74	0.62	0.33	0.31	0.60	0.22						
Irt1	1.90	1.45	0.57	0.57	1.51	1.23	0.91	1.09	1.02	0.53	0.43	0.75	0.97	0.78	1.04	1.04	1.64	1.19	1.41	1.94	0.69						
Irt2	2.03	1.59	0.25	0.60	1.34	1.41	1.15	1.25	0.67	0.37	0.67	0.57	0.88	0.83	1.44	1.44	1.08	1.13	1.78	2.61	1.09						
Irt3	1.49	0.86	1.17	0.58	0.58	0.85	0.55	0.45	0.21	0.82	5.02	1.64	0.40	0.26	0.36	0.36	0.74	0.73	0.65	0.27	0.41						
Irt4	1.50	1.12	0.44	0.38	0.92	1.47	0.52	0.58	0.30	0.41	0.43	0.56	0.44	0.30	0.88	0.88	2.66	0.87	0.92	0.76	0.36						
Irt5	1.53	1.12	0.45	0.28	0.86	1.52	0.47	0.43	0.39	0.56	0.40	0.73	0.44	0.21	0.75	0.75	2.78	0.94	1.03	0.80	0.49						
Irt6	1.77	1.34	0.66	0.29	0.45	1.24	0.70	0.84	0.81	0.44	0.38	0.79	0.87	0.53	0.70	0.70	2.74	1.28	0.90	0.79	0.51						
Irt7	1.79	1.36	0.61	0.49	0.42	1.28	0.75	0.80	0.81	0.54	0.35	0.91	0.91	0.55	0.79	0.79	2.75	1.34	1.07	0.81	0.61						
Irt8	1.69	1.29	0.60	0.24	1.28	1.44	0.62	0.63	0.47	0.53	0.59	0.82	0.72	0.56	0.68	0.68	1.30	0.96	1.06	0.64	0.43						
Irti	1.93	1.39	0.85	0.75	1.65	2.03	1.03	1.11	1.41	0.67	4.35	0.64	0.75	0.72	0.83	0.83	0.96	1.21	1.94	2.89	0.91						
Itrt	1.73	1.22	0.97	0.47	1.90	1.64	1.98	1.06	0.63	0.48	1.45	0.59	0.70	0.93	1.43	1.43	1.06	1.31	1.41	1.58	0.51						
Ivrt	0.00	0.00	0.00	0.00	0.00	0.00	0.00	0.00	0.00	0.00	0.00	0.00	0.00	0.00	0.00	0.00	0.00	0.00	0.00	0.00	0.00	0.00	0.00	0.00	0.00	0.00	0.00
Ivru	0.92	0.51	0.74	0.26	0.55	0.88	0.48	0.83	0.44	0.20	0.22	0.35	0.44	0.41	0.29	0.29	0.39	1.28	0.30	0.38	0.08	0.00	0.00	0.00	0.00	0.00	0.00
mean RMSD	1.59	1.13	0.63	0.44	1.14	1.26	0.84	0.89	0.67	0.45	1.12	0.75	0.61	0.51	0.82	0.82	1.49	1.14	1.16	1.30	0.63	0.00	0.00	0.00	0.00	0.00	0.00

^a RMSD values for the wild-type RT calculated for all heavy atoms and only backbone atoms for the 20 Å core. Local residue flexibility is also reported for all the residues in a 5 Å core of NNBS. RMSD values are referred to 1VRT.

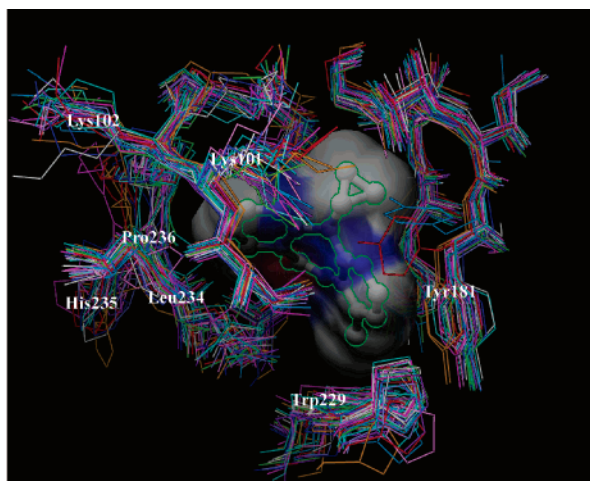


Figure 3. Flexibility of the NNBS. A 5 Å core of residues from nevirapine (1VRT) is displayed. The higher flexibility of Lys101, Lys102, Tyr181, Trp229, Leu234, His235, and Pro236 residues is clearly visible.

(mean $\text{RMSD}_{\text{backbone}} = 1.13 \text{ \AA}$) indicates that the overall wild-type structure does not undergo significant backbone movements upon binding of diverse ligands. On the other hand, a greater NNBS movement is observed on the side chains (mean $\text{RMSD}_{\text{all atoms}} = 1.59$) upon ligand binding. Deeper inspection of the RMSD values calculated on the single amino acids suggests that the more flexible side chains are those connected to Lys101, Lys102, Tyr181, Trp229, Leu234, His235, and Pro236 whose RMSDs were calculated to be higher than a threshold value of 1 Å (Table 3 and Figure 3). For further information the reader is referred to a recent extensive study in the structural rearrangement and ligand-induced fit of HIV-RT reported by Lawtrakul et al.⁷

In view of the above RT flexibility, inclusion of such structural variability in a docking study becomes of fundamental importance. The ideal situation would be a program able to dock a ligand into a protein structure from a different complex easily and with reasonable accuracy. This has been referred to as “cross-docking”.^{19,60} There are a number of ways that the issue of local flexibility can be approached when applied to systems with only small induced-fit effects. Different docking methods and the ways in which they accommodate protein flexibility may be found elsewhere.⁶¹ Autodock 3.0.5 (version 4.0⁶² with protein flexibility has been announced to be released soon) as well as many other molecular docking programs is not able to consider the protein flexibility. To overcome this limitation we performed an extensive cross-docking study in order to check if different ligands can still bind different NNBS at a low energy level.

To quantify the ligand docking quality, the docking accuracy (DA) function was used,^{23,63} which makes use of RMSD values and measures how accurately the ligands are docked

$$\text{DA} = \text{frmsd} \leq a + 0.5 (\text{frmsd} \leq b - \text{frmsd} \leq a) \quad (1)$$

where $\text{frmsd} \leq a$ indicates the fraction of ligands docked into a given receptor with RMSD less than or equal to $a \text{ \AA}$. The docking accuracy is zero if $\text{frmsd} \leq b$ is zero.

As previously indicated by Vieth et al., correctly docked conformations are those with less than 2 Å RMSD on all atoms from the crystallographic structure of the ligand in the ligand/receptor complex. Structures with a RMSD value larger than 4 Å were considered incorrectly docked or misdocked. Structures with RMSD between 2 and 3 Å were considered partially docked, whereas those with RMSD between 3 and 4 Å were partially misdocked and not considered in the DA calculation.

Each ligand was docked in each of the 27 wild-type NNRTI binding sites. The RMSD between the coordinates of the docked ligands and the coordinates in their native crystal structure was calculated. For this purpose the backbone atoms of each generated complex were superimposed onto the corresponding atoms of the native crystal structure. The RMSD was calculated for the ligand atoms only, taking into account possible local symmetries of the ligands. The average RMSD between the 20 Å binding pocket structures is 1.13 Å for the backbone atoms and 1.58 Å for all heavy atoms. Similar to what was found by Daeyaert,²⁷ the average RMSD between the binding pocket atoms in the Macromodel-minimized complexes and the original binding pockets was very low (0.2 Å), indicating that the complexes are rather stable and that it is reasonable to consider the RMSD values for the ligand atoms only. The results are presented in matrix form in Tables 4 and 5. Each entry gives the result of the docking of the ligand (figuring in the row header) into the binding site (figuring in the column header). The diagonal entries in Tables 4 and 5 are the RMSDs found when the ligands are docked into their native binding sites (see previous section for details). The off-diagonal entries in Tables 4 and 5 mimic the predictive docking of newly designed ligands into the binding pocket of a ligand with known crystal structure.

As already outlined in the previous paragraph, in general, the best cluster selection criteria gave the best results, having an average DA value of 0.75 higher than that of the best docked (DA = 0.64). Analogously, the number of correctly docked conformations was also higher for the best cluster selection (average number of correctly docked conformations = 17.8) than those obtained by the best docked criteria (average number of correctly docked conformations = 12.4). Furthermore, considering either the docking of the inhibitors in the same protein or the docking of the same inhibitor in the different proteins in 23 and 22 out of 27 cross-docking experiments, respectively, the best cluster conformation selection performed better (higher DA values) than the best docked conformation selection. In those cases where a decrease occurred, the absolute differences of the DA values between the two selection methods were comprised in the range of only 0.02–0.09.

As an example, the DA improvement upon the best cluster conformation choice is evident in the 1EP4 NNBS, which seems to be highly susceptible to the induced fit from the highly flexible native ligand (S-1153). In fact, using the best cluster conformation selection, 14 out of 27 inhibitors were correctly docked in 1EP4 NNBS, while using the best docked conformation selection only 9 conformations were found correctly docked. On the other hand, from the point of view of

Table 4. Matrix of RMSDs Obtained by Cross-Docking 27 NNRTIs into 27 Wild-type HIV-RT Binding pockets. Values are from the Best Docked Conformations (First Ranked)

		Proteins																											
		IBQM	IC0T	IC0U	IC1B	IC1C	IDTQ	IDTT	IEET	IEP4	IFK9	IHNI	IHNV	IJLQ	IKLM	IREV	IRTI	IRT2	IRT3	IRT4	IRT5	IRT6	IRT7	IRTH	IRTI	ITVR	IVRT	IVRU	DA
Ligands	IBQM	1.53	2.39	1.38	1.60	1.66	1.39	1.38	1.38	1.94	1.06	2.37	2.43	2.52	5.26	1.81	1.74	1.61	2.04	1.88	1.94	1.02	2.54	2.39	1.71	1.53	2.13	2.34	0.80
	IC0T	2.24	2.38	0.89	1.03	1.79	2.34	2.23	2.28	3.02	0.89	2.15	2.27	2.26	0.82	2.77	0.83	2.46	1.93	2.48	2.49	2.13	2.84	2.19	2.79	2.59	3.12	2.75	0.59
	IC0U	1.95	2.52	2.35	1.06	2.41	1.15	2.05	1.08	1.59	2.06	2.64	2.15	1.97	0.89	2.30	2.64	0.72	2.03	2.60	2.63	2.39	1.59	1.95	3.49	2.35	2.68	2.27	0.67
	IC1B	2.60	0.86	0.99	0.82	0.99	1.00	0.93	2.27	1.02	2.35	1.52	0.95	0.92	1.21	1.12	1.11	0.96	1.85	1.42	1.43	0.76	1.54	0.88	1.34	1.40	1.40	1.08	0.94
	IC1C	1.87	0.79	1.07	1.01	1.16	1.21	2.77	1.84	1.12	1.33	1.12	1.74	1.09	1.22	1.36	1.35	0.97	3.09	1.44	2.68	1.04	1.68	0.87	1.27	1.26	1.42	1.29	0.93
	IDTQ	1.67	1.54	1.57	3.59	2.78	1.44	1.46	1.55	3.39	1.99	4.87	1.56	1.49	2.97	4.55	7.20	1.58	2.86	1.93	2.00	1.41	1.79	2.12	3.87	3.49	2.95	3.04	0.59
	IDTT	4.06	2.35	1.68	1.30	2.89	1.55	1.49	1.44	3.33	1.27	3.01	1.82	1.62	4.13	2.26	1.41	1.68	3.85	1.93	1.69	1.35	1.93	2.74	2.93	5.29	1.92	2.02	0.67
	IEET	3.26	1.00	1.78	1.19	1.90	1.64	0.98	1.06	3.32	2.09	2.16	2.11	0.71	4.80	2.07	2.22	3.54	3.68	1.91	2.06	1.74	2.78	1.26	4.12	2.11	2.41	2.69	0.59
	IEP4	2.87	3.53	8.20	7.11	2.62	2.78	2.66	2.65	0.89	4.23	4.58	3.64	3.38	4.37	3.33	3.03	2.58	3.04	5.04	3.39	3.23	3.24	5.32	1.41	3.70	8.21	3.65	0.19
	IFK9	1.28	0.93	0.82	1.03	2.52	3.79	1.18	1.17	1.38	0.35	0.92	3.75	1.12	0.87	3.80	0.75	1.13	1.79	1.24	1.19	0.85	2.09	3.71	1.50	3.02	3.03	1.16	0.76
	IHNI	1.91	1.29	2.35	1.38	2.30	1.70	2.19	1.97	2.96	1.02	0.61	2.28	1.44	2.14	2.22	2.32	2.49	10.10	1.51	1.73	1.96	2.20	0.79	2.02	2.24	1.59	1.49	0.74
	IHNV	0.97	1.28	1.10	1.43	2.79	1.26	1.20	1.30	2.98	1.08	0.73	1.20	1.14	2.91	1.66	2.63	2.59	1.97	1.47	1.63	1.09	2.71	2.48	3.43	2.51	2.12	1.39	0.80
	IJLQ	2.68	1.84	2.73	2.09	3.06	2.64	2.45	2.51	3.20	1.83	2.14	2.63	0.90	1.14	2.87	2.91	2.95	3.01	2.69	2.92	2.35	4.43	1.91	3.08	2.78	1.56	1.86	0.56
	IKLM	5.70	5.67	5.90	2.02	1.94	6.00	5.91	3.63	2.07	5.92	5.28	3.84	6.93	1.42	5.89	2.07	2.41	6.50	6.04	5.75	6.06	5.52	5.73	1.81	2.01	5.72	6.31	0.20
	IREV	1.65	1.65	1.66	1.70	1.31	1.65	1.61	1.41	5.30	1.37	1.50	1.37	2.82	1.82	1.00	3.13	2.98	1.84	1.14	1.41	1.35	1.04	2.71	1.81	3.01	1.25	2.94	0.81
	IRTI	1.76	1.00	1.14	1.50	1.11	1.05	2.43	2.31	1.04	1.03	1.36	1.89	2.07	1.15	2.29	0.90	1.13	3.12	1.40	1.61	0.94	1.60	1.90	2.39	1.73	1.24	1.17	0.87
	IRT2	1.41	1.91	2.01	1.11	1.12	2.10	2.05	2.06	2.14	2.38	2.79	2.11	2.23	1.08	2.85	0.87	0.99	2.81	2.74	2.11	1.88	2.84	2.26	1.85	1.81	4.02	2.31	0.67
	IRT3	3.42	2.60	3.16	3.33	3.04	2.72	2.50	2.98	3.16	2.51	2.77	3.59	2.99	2.99	2.65	3.25	3.34	0.83	2.12	2.97	2.90	1.82	2.64	3.35	3.41	2.02	2.48	0.35
	IRT4	1.97	1.77	1.77	1.97	1.91	1.76	1.64	2.28	6.94	1.40	3.02	1.92	1.60	3.58	3.00	1.91	1.77	2.26	1.16	1.22	1.71	2.09	1.63	2.21	1.91	2.99	1.58	0.76
	IRT5	1.76	1.66	1.54	1.92	2.15	1.61	1.60	1.83	1.94	1.35	1.60	1.67	2.00	3.91	2.21	2.10	2.06	1.99	0.91	0.81	1.44	1.97	1.47	2.42	1.82	1.62	1.45	0.87
	IRT6	2.32	3.03	1.63	1.86	2.81	2.79	1.83	2.83	3.33	1.62	2.89	2.55	1.68	3.33	2.92	3.03	3.13	2.95	1.81	3.11	1.57	1.66	1.66	2.94	2.89	2.69	2.92	0.56
	IRT7	2.42	2.78	2.01	2.39	3.60	3.07	3.00	2.80	3.26	1.96	3.33	2.90	2.88	3.73	3.02	4.69	4.06	2.35	1.66	3.33	1.84	1.30	1.91	3.68	4.03	1.42	2.61	0.39
	IRTH	2.78	0.88	2.44	2.63	2.53	2.17	1.26	2.96	3.29	2.03	1.91	2.37	2.07	2.21	2.36	2.58	2.66	2.21	3.18	2.11	2.38	2.27	1.16	2.62	2.83	1.36	1.19	0.57
	IRTI	2.46	1.12	1.27	1.61	2.95	2.17	2.49	2.00	2.83	2.89	1.28	2.19	0.96	1.38	2.82	1.60	2.94	2.16	2.42	2.61	2.52	1.86	2.21	1.51	2.17	2.27	2.79	0.69
	ITVR	3.05	0.67	0.90	1.21	3.07	1.00	1.12	1.14	3.82	0.72	0.81	1.04	0.93	1.22	2.05	0.72	2.89	1.73	1.44	1.53	0.85	3.01	2.62	2.94	3.05	3.29	0.82	0.70
	IVRT	3.02	1.98	2.50	2.75	2.71	1.44	2.56	2.66	3.43	2.29	2.69	2.66	2.51	2.62	2.35	2.73	3.08	2.12	2.35	2.56	2.46	1.48	2.40	2.96	2.89	2.10	2.32	0.50
	IVRU	1.61	2.16	2.10	1.55	2.37	2.42	2.45	2.72	1.69	1.31	2.92	1.51	2.00	2.09	1.84	2.88	1.46	10.27	2.37	2.77	2.27	1.93	2.21	2.36	2.50	1.06	2.07	0.65
DA.	0.63	0.78	0.76	0.81	0.63	0.74	0.72	0.74	0.43	0.80	0.61	0.65	0.76	0.59	0.52	0.59	0.63	0.50	0.76	0.65	0.80	0.72	0.69	0.56	0.48	0.63	0.67		

RMSD < 1 | 1 < RMSD < 2 | 2 < RMSD < 3 | 3 < RMSD < 4 | 4 < RMSD < 5 | RMSD > 5

Table 5. Matrix of RMSDs Obtained by Cross-Docking 27 NNRTIs into 27 Wild-type HIV-RT Binding Pockets. Values are from the Best Cluster Conformations

		Proteins																											
		IBQM	IC0T	IC0U	IC1B	IC1C	IDTQ	IDTT	IEET	IEP4	IFK9	IHNI	IHNV	IJLQ	IKLM	IREV	IRTI	IRT2	IRT3	IRT4	IRT5	IRT6	IRT7	IRTH	IRTI	ITVR	IVRT	IVRU	DA
Ligands	IBQM	1.53	1.35	1.38	1.60	1.66	1.39	1.38	1.38	2.06	1.06	1.01	1.38	1.28	1.77	1.81	1.74	1.61	7.98	1.88	1.94	1.02	1.86	1.43	1.71	1.53	2.13	1.44	0.93
	IC0T	2.24	0.86	0.89	1.03	0.65	1.20	0.80	2.28	1.46	0.89	1.15	2.20	0.87	0.82	1.43	0.83	0.59	1.93	1.22	1.24	0.41	1.72	0.85	1.07	2.59	1.57	1.18	0.93
	IC0U	1.95	1.14	0.86	1.06	1.62	1.15	0.91	1.08	1.59	1.07	1.38	2.15	1.97	0.89	2.30	0.96	0.72	2.03	1.18	1.41	0.68	1.59	0.92	1.36	2.58	1.80	1.93	0.93
	IC1B	2.27	0.86	0.99	0.82	0.99	1.00	0.93	1.02	1.02	9.92	1.52	0.95	0.92	1.21	1.12	1.11	0.96	2.58	1.42	1.43	0.76	1.54	0.88	1.34	1.40	1.40	1.08	0.93
	IC1C	1.24	0.79	1.07	1.01	1.16	1.21	1.12	1.71	1.12	1.33	1.12	1.00	1.09	1.22	1.36	1.35	0.97	2.18	1.44	1.41	1.04	1.68	0.87	1.27	1.26	1.42	1.29	0.98
	IDTQ	5.43	10.54	1.57	3.59	1.46	2.23	1.46	1.55	4.85	10.23	9.46	1.56	9.80	7.87	2.19	1.74	7.29	9.01	1.93	2.00	1.41	1.79	0.77	2.52	2.55	2.89	1.84	0.52
	IDTT	1.67	1.09	1.19	1.30	1.64	1.39	0.85	1.14	5.07	1.27	9.85	1.82	0.97	2.46	2.26	7.72	1.30	3.85	1.46	1.62	1.48	1.42	1.20	2.19	1.49	3.72	2.34	0.74
	IEET	1.94	1.92	1.78	1.19	1.30	1.11	0.98	1.06	2.84	9.27	10.80	1.12	11.89	8.08	2.07	1.17	3.29	10.08	1.79	4.16	1.22	2.11	1.26	2.87	2.11	2.04	1.86	0.63
	IEP4	7.24	7.77	7.86	7.11	8.42	7.59	7.24	7.29	0.89	7.61	6.60	6.37	7.10	5.08	6.35	6.78	7.42	6.62	6.52	3.39	7.14	6.67	8.42	7.98	6.43	7.58	7.62	0.04
	IFK9	1.28	0.93	0.82	1.03	0.99	0.97	1.18	1.17	1.38	0.35	0.92	0.96	1.12	0.87	1.68	0.75	1.13	1.79	1.24	1.19	0.85	2.09	1.14	1.50	1.12	2.03	1.16	0.96
	IHNI	0.97	1.29	1.34	1.38	11.45	10.02	2.19	1.52	2.34	1.02	0.61	0.93	1.44	6.97	1.92	1.28	8.50	8.20	1.51	1.73	1.00	1.64	0.79	8.70	9.97	1.59	1.49	0.70
	IHNV	0.97	1.28	1.10	1.43	1.09	1.26	1.20	1.30	1.10	1.08	0.73	1.20	1.14	8.41	1.66	0.90	1.14	1.97	1.47	1.63	1.09	1.78	1.13	1.83	1.01	2.12	1.39	0.94
	IJLQ	0.55	0.88	1.05	2.09	2.13	2.25	2.45	1.66	3.20	0.81	1.71	0.96	0.90	1.14	1.29	3.24	1.80	3.08	1.44	1.49	1.09	1.62	1.91	3.08	2.55	1.56	0.72	0.76
	IKLM	4.34	4.35	5.70	2.02	1.94	5.95	4.86	3.63	2.07	5.72	5.28	5.28	5.24	1.42	5.46	2.07	1.74	6.50	4.52	4.44	5.54	5.17	5.17	1.81	2.01	5.26	5.65	0.22
	IREV	1.65	1.65	1.66	1.70	1.31	1.65	1.61	1.41	1.76	1.37	1.50	1.37	1.73	8.98	1.00	1.51	1.96	1.84										

Table 6. Matrix of RMSDs Obtained by Cross-Docking 14 NNRTIs into 14 Mutated HIV-RT Binding Pockets. Values are from the Best Docked Conformations (First Ranked)

		Proteins													
		1BQN	1FK0	1FKP	1IKV	1IKW	1IKX	1IKY	1JKH	1JLA	1JLB	1JLC	1JLF	1JLG	1UWB
Ligands	1BQN	1.18	1.31	2.39	1.27	1.27	2.30	1.27	1.18	1.92	1.34	1.49	1.48	1.26	2.51
	1FK0	4.84	0.41	0.82	1.04	0.71	3.50	0.95	0.79	1.21	0.81	0.94	1.18	1.33	3.57
	1FKP	3.07	1.94	1.06	3.07	1.42	1.21	2.08	1.09	3.82	1.21	1.48	2.10	1.06	2.31
	1IKV	5.01	0.88	0.91	0.33	0.52	3.59	0.79	0.80	1.13	0.72	1.18	1.05	1.10	3.83
	1IKW	3.85	0.66	0.87	0.62	0.30	3.54	0.92	0.68	1.12	0.88	1.12	3.66	0.95	3.71
	1IKX	4.49	3.37	0.67	2.31	0.88	0.89	2.65	0.81	3.02	0.85	3.44	3.33	0.59	2.88
	1IKY	3.30	2.52	1.43	2.27	3.47	1.19	1.15	1.12	3.94	1.43	1.15	1.53	1.21	3.36
	1JKH	3.87	0.89	3.32	1.08	1.12	3.20	1.53	0.86	1.40	0.91	1.24	1.03	1.44	3.27
	1JLA	2.36	6.31	2.49	1.73	2.23	2.40	2.47	2.08	1.03	2.15	1.83	1.61	2.61	2.34
	1JLB	3.20	1.94	1.54	2.86	2.51	1.48	2.64	1.41	3.99	1.41	1.83	2.07	2.20	1.86
	1JLC	3.69	1.54	1.36	3.11	1.39	1.79	1.53	1.73	4.48	2.05	1.77	1.56	2.36	2.39
	1JLF	3.11	1.89	1.21	0.62	1.50	2.04	1.02	1.24	2.52	1.20	1.58	1.24	1.23	2.24
	1JLG	3.74	2.03	1.03	1.26	1.24	2.63	1.95	1.19	1.43	1.45	1.61	2.69	1.26	1.49
	1UWB	3.16	2.28	1.33	2.98	1.17	1.18	2.96	1.10	2.95	1.06	2.95	0.86	1.17	0.61
D.A.	0.10	0.74	0.85	0.70	0.85	0.56	0.81	0.96	0.57	0.92	0.89	0.74	0.89	0.41	

RMSD < 1 1 < RMSD < 2 2 < RMSD < 3 3 < RMSD < 4 4 < RMSD < 5 RMSD > 5

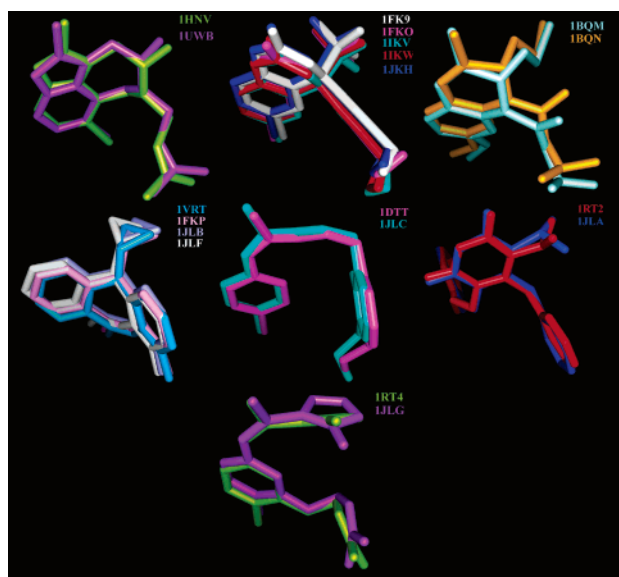
tially misdocked, and 17 misdocked) to the best cluster conformation selection (4 correctly docked, 4 partially docked, 1 partially misdocked, and 18 misdocked).

Data in Tables 4 and 5 allow also the virtual comparison of a classical docking study (many ligands against a single site) versus the cross-docking study (many ligands docked into several sites). In fact, if one considers the panel of the 27 ligands cocrystallized in the wild-type RTs as a set of newly designed anti-RT candidates, applying the classical docking approach the risk of uncorrected binding mode is definitely higher (from 1 to 13 and 2 to 14 for the best docked and best cluster conformations, respectively) than using the cross-docking approach in which the different NNRTI binding pockets allow each ligand to adopt different poses that seem to converge to that experimentally observed (in 23 out of the 27 ligands more than 50% is correctly docked in the 27 sites for both the best docked and best cluster conformations).

While this paper was in preparation we also studied application of the cross-docking approach which led to disclosing the binding mode of a series of anti-RT indolyl aryl sulfones (IAS).^{64,65} In this paper the Merck lead compound L-737126 was docked against 14 RTs. In all cases, the docked conformations (either the best cluster or the best docked conformations) were in good agreement with each other, identifying a unique binding mode for L-737126 and confirming the usefulness of the cross-docking approach. Moreover, the use of the Autodock program allowed the structure-based alignment of 70 IASs derivatives to develop a predictive 3D QSAR model, which was used as a tool to design new potent anti-HIV compounds.

Mutated RTs. In parallel to the previously discussed studies on the wild-type RTs, cross-docking experiments were also conducted on the mutated RT set.

Observing NNRTI-bound conformations in the wild-type or mutated RT forms, it seems that for ligands also able to inhibit the RT mutants a unique binding mode exists for both enzymes. This observation is supported by the low RMSD (Figure 4) values between wild-type and mutated bound conformations for 8CI-TIBO

**Figure 4.** Examples of superimposed NNRTI-bound conformations in either wild-type or mutated RTs (see Table 1 for details).

(RMSD_{1HNW-1UWB} = 0.365), efavirenz (RMSD_{1FK9-1FK0} = 0.969; RMSD_{1FK9-1IKV} = 1.122; RMSD_{1FK9-1IKW} = 1.000; RMSD_{1FK9-1JKH} = 0.324), Hby097 (RMSD_{1BQM-1BQN} = 0.681), nevirapine (RMSD_{1VRT-1FKP} = 0.330; RMSD_{1JLB-1JLF} = 0.543; RMSD_{1VRT-1JLF} = 0.736), PETT 130A94 (RMSD_{1DTT-1JLC} = 0.391), TNK-651 (RMSD_{1RT2-1JLA} = 0.362), and UC-781 (RMSD_{1RT4-1JLG} = 0.526). Thus, parallel cross-docking experiments on both wild-type and mutated RT would be a useful tool for SBDD studies to design new inhibitors able to tightly bind both enzymes.

Each ligand found in the RT-mutated crystals was docked in the 14 mutated enzyme similar to the previous section mimicking the SBDD of new ligands active against RT mutants.

The results are presented in matrix form in Tables 6 and 7. Each entry gives the result of the docking of the ligand (figuring in the row header) into the binding site

Table 7. Matrix of RMSDs Obtained by Cross-Docking 14 NNRTIs into 14 Mutated HIV-RT Binding Pockets. Values are from the Best Cluster Conformations

		Proteins													
		IBQN	IFKO	IFKP	IKV	IKW	IKX	IKY	IJKH	IJLA	IJLB	IJLC	IJLF	IJLG	IUW
Ligands	IBQN	1.45	1.31	1.25	1.27	1.27	1.54	1.27	1.18	1.92	1.34	1.49	1.48	1.26	1.17
	IFKO	1.27	0.41	0.82	1.04	0.71	0.84	0.95	0.79	1.21	0.81	0.94	1.18	1.33	0.82
	IFKP	3.07	1.05	1.06	0.93	1.42	1.21	1.09	1.09	1.08	1.21	1.48	2.10	1.06	1.41
	IKV	1.45	0.88	0.91	0.33	0.52	0.83	0.79	0.80	1.13	0.72	1.18	1.05	1.10	0.56
	IKW	1.32	0.66	0.87	0.62	0.30	0.83	0.92	0.68	1.12	0.88	1.12	0.84	0.95	0.71
	IKX	4.49	1.60	0.67	2.31	0.88	0.89	1.43	0.81	2.15	0.85	1.07	0.99	0.59	1.14
	IKY	1.45	9.48	1.43	1.26	1.59	1.19	1.15	10.34	1.35	9.05	1.15	1.53	1.21	1.88
	IJKH	1.69	0.89	1.09	1.08	1.12	1.10	1.53	0.86	1.40	0.91	1.24	1.03	1.44	0.96
	IJLA	1.97	6.74	6.17	1.73	6.35	6.20	2.47	6.50	1.03	6.12	2.01	1.61	5.42	2.34
	IJLB	3.20	1.94	1.54	0.70	0.70	1.48	1.13	1.41	1.49	1.41	1.83	0.98	1.52	1.58
	IJLC	1.42	1.27	1.36	3.47	1.39	1.79	1.53	1.07	2.28	2.05	1.36	1.28	1.42	2.88
	IJLF	3.11	1.28	1.21	0.62	1.50	1.21	1.02	1.24	1.19	1.20	1.58	1.24	1.23	1.45
	IJLG	1.98	1.44	1.03	1.68	1.68	1.29	1.95	1.19	1.43	1.45	1.61	1.29	1.26	1.49
	IUWB	3.17	2.28	1.33	1.38	1.17	1.18	0.87	1.10	1.03	1.06	0.92	0.86	1.17	0.61
D.A.	0.64	0.82	0.93	0.89	0.93	0.93	0.96	0.86	0.93	0.82	0.96	0.96	0.93	0.93	

RMSD < 1	1 < RMSD < 2	2 < RMSD < 3	3 < RMSD < 4	4 < RMSD < 5	RMSD > 5
----------	--------------	--------------	--------------	--------------	----------

(figuring in the column header). The diagonal entries in Tables 6 and 7 are the RMSDs found when the ligands are docked into their native binding sites (see previous section for details). The off-diagonal entries in Tables 6 and 7 mimic the predictive docking of newly designed ligands into the binding pocket of a ligand with known crystal structure. Again, compared to the best docked conformation selection, the best cluster method proved to be more efficient, reaching an average DA value of 0.89. In only three cases the best cluster selection afforded inferior DA values; these are the 1JLA ligand docked into the different mutated proteins and all the ligands docked into the 1JKH and 1JLB proteins (Tables 6 and 7); nevertheless, in the latter the DA values were only marginally decreased (about 10%), while for TNK-651 (1JLA) its high flexibility could be the reason for alternate binding mode selected by the best cluster method.

These results are even more encouraging than those obtained from the previous cross-docking studies. In fact, Autodock was able to correctly dock the NNRTI into the mutated RTs with higher efficiency, thus demonstrating that it is a suitable tool for SBDD and docking of new ligands into the wild-type and mutated RT forms. Moreover, it could be also applied to gain insight on the mode of action (based on its ability to reproduce the most profitable orientations/conformations of binding) of new NNRTI active toward both the wt and mutated forms of RT.

Conclusions

We presented an evaluation of the Autodock program for the docking of ligands into the nonnucleoside binding pocket of HIV-1 reverse transcriptase. Autodock proved to efficiently reproduce, under a threshold RMSD value of 2.0 Å, 98% of the NNRTI-bound conformations in their native NNBSs. Moreover, to address the important issue on the NNBS conformational flexibility, cross-docking experiments conducted by docking 41 NNRTIs into 41 different RTs (full tables are available in the Supporting Information) proved the Autodock program to be a useful tool for structure-based drug design in developing new anti-RT agents active against wild-type

and mutated forms of the enzyme and for exploring (in terms of their preferential orientations/conformations within the binding site) the mode of action of such compounds. To support our results, we recently applied the cross-docking approach to define in a unique way the binding mode of the L-737126 lead compound and design new and potent anti-HIV IASs derivatives. Application of a cross-docking study on using mutated RTs to design anti-HIV agents active against resistant strains is underway and will be reported soon.

Materials and Methods

Structures Preparation. Forty-one publicly available X-ray crystal structures of reverse transcriptase complexed with a NNRTI were retrieved from the Protein Data Bank⁶⁶⁻⁶⁸ (Table 1). Of the 41 complexes, 27 belonged to the wild-type enzyme [because the long distance from the NNBS, the tetramutant 1RT3 and the C280S mutated forms were considered as wild-type RT, Table 1] and 14 to RT mutated forms. For the cross-docking studies all the complexes were superimposed on each other arbitrarily using nevirapine/RT (1VRT) as reference complex. The superimposition of the RT complexes was performed by means of the program ProFit version 2.2⁶⁹ using the implemented McLachlan algorithm;⁷⁰ all residue's backbone atoms comprised in a 20 Å core from nevirapine (1VRT) were selected with the Chimera program⁷¹ (182 residues) and used as reference for the fitting; the same number of residues (Trp88A-Tyr115A, Ser156A-Leu210A, Trp212A, Leu214A-Ile244A, Lys263A, Asn265A-Tyr271A, Glu312A-Ile326A, Tyr339A-Thr351A, Ile375A, Thr377A-Lys385A, Gln23B, Pro25B-Glu28B, Ile31B-Lys32B, Val35B, Thr131B-Arg143B) was used for all complexes superimpositions. The above aligned protein/ligand complexes were prepared uniformly for docking in order to minimize introduction of bias. First, to reduce CPU time, each complex was reduced to a smaller size by removing solvent and any residues atoms out 20 Å from the cocrystallized ligands. Then, using the MacroModel program, the complexes were minimized to alleviate steric contacts which usually arise due to the random way in which hydrogens are added to the heavy atoms. Hydrogens were added to the receptors and ligands with the Maestro program.⁷² Protonation states were assumed to be those most common at pH 7, i.e., lysines, arginines, aspartates, and glutamates were considered in the ionized form.

During the minimization water and any ions in the crystal structures of the complex were left with the receptor. It was our intent to simply relieve steric contacts created from this

addition, not to have large conformational changes occur during minimization. The criteria used to set up the minimization helps to ensure that this was the case. The minimizer used was the batchmin minimizer distributed with MacroModel.⁷³ Several force field implementations are available with this minimizer, and we used the Amber⁷⁴ all-atom implementation. This force field was selected because it was generally well parametrized for most of our complexes. The setup criteria for the minimization basically involved selecting an 8 Å core of atoms around the ligand for minimization and a 10 Å shell of atoms surrounding that to be used for long-range electrostatic interactions during the minimization. Atoms in the ligand and selected core of the receptor underwent the full minimization process. Atoms in the shell surrounding this were fixed in place, but charges were placed on them by the minimizer to be used for nonbonded electrostatic interactions with atoms in the core and ligand. Atoms beyond the shell were ignored. The minimizations were run with a gradient convergence of 0.1 and an iteration limit of 20 000 for all complexes. A solvation model was not used; however, in many cases numerous waters from the crystal structures were included in the core and shell. Minimizations were run on an IBM-compatible PC equipped with an AMD 3GHz CPU, running the SUSE 9.0 distribution of Linux.

Once the minimizations were complete, the ligands and the receptors were extracted into separate files to be used for the subsequent docking set up.

Docking Setup. Autodock 3.0.5²² was used for all docking calculations. Several detailed studies by the McCammon group on binding modes and affinity of HIV-1 integrase inhibitors have shown that the estimated free energies from the Autodock program are in good agreement with the available experimental values.⁷⁵ Prior to any docking, to eliminate any possibility of biasing the docking experiments, the ligand-bound conformations were extracted from the minimized complexes and energy minimized using the following protocol: each molecule was energy minimized to a low gradient. The nonbonded cutoff distances were set to 20 Å for both van der Waals and electrostatic interactions. An initial random velocity to all atoms corresponding to 300 K was applied. Three subsequent molecular dynamics runs were then performed. The first was carried out for 10 ps with a 1.5 fs time step at a constant temperature of 300 K for equilibration purposes. Next, molecular dynamics was carried out for 20 ps, during which the system is coupled to a 150 K thermal bath with a time constant of 5 ps. The time constant represents approximately the half-life for equilibration with the bath; consequently, the second molecular dynamics command caused the molecule to slowly cool to approximately 150 K. The third and last dynamic cooled the molecule to 50 K over 20 ps. A final energy minimization was then carried out for 250 iterations using conjugate gradient. The minimizations and molecular dynamics were in all cases performed in simulated aqueous solution using the batchmin GBSA keyword. The AutodockTools package was employed to generate the docking input files and analyze the docking results; the same procedures as those described in the manual were followed. All the nonpolar hydrogens and the water molecules were removed. The Kollmann charges were loaded for the proteins, while the all atom amber charges applied by the MacroModel program were retained in the ligand. A grid box size of 61 × 81 × 61 points with a spacing of 0.375 Å between the grid points was implemented and covered more than 8 Å of the NNBS. The grid was centered on the mass center of the experimentally bound nevirapine (1VRT) coordinates taken as NNRTI representative. For all the inhibitors the single bonds including the amide bonds were treated as active torsional bonds (see all structures in Table 1). Thirty docked structures, i.e., 30 runs, were generated by using genetic algorithm searches. A default protocol was applied, with an initial population of 50 randomly placed individuals, a maximum number of 2.5 × 10⁵ energy evaluations, and a maximum number of 2.7 × 10⁴ generations. A mutation rate of 0.02 and a crossover rate of 0.8 were used. Results differing by less than 2.0 Å in positional root-mean-

square deviation (RMSD) were clustered together and represented by the result with the most favorable free energy of binding. The RMSD values reported in this work are based upon all atom comparisons between the docked structures and the initial structures of the inhibitors.

Acknowledgment. Financial support provided by the Research Training Network (LS HG-CT-2003-503480) is gratefully acknowledged.

Supporting Information Available: A matrix of RMSDs obtained by full cross-docking simulations. This material is available free of charge via the Internet at <http://pubs.acs.org>.

References

- (1) Davey, R. T., Jr.; Dewar, R. L.; Reed, G. F.; Vasudevachari, M. B.; Polis, M. A.; Kovacs, J. A.; Falloon, J.; Walker, R. E.; Masur, H.; et al. Plasma viremia as a sensitive indicator of the antiretroviral activity of L-697661. *Proc. Natl. Acad. Sci. U.S.A.* **1993**, *90*, 5608–5612.
- (2) Wallace, R. G. AIDS in the HAART era: New York's heterogeneous geography. *Soc. Sci. Med.* **2003**, *56*, 1155–1171.
- (3) De Clercq, E. The role of non-nucleoside reverse transcriptase inhibitors (NNRTIs) in the therapy of HIV-1 infection. *Antiviral Res.* **1998**, *38*, 153–179.
- (4) Pedersen, O. S.; Pedersen, E. B. Non-nucleoside reverse transcriptase inhibitors: the NNRTI boom. *Antiviral Chem. Chemother.* **1999**, *10*, 285–314.
- (5) Campiani, G.; Ramunno, A.; Maga, G.; Nacci, V.; Fattorusso, C.; Catalanotti, B.; Morelli, E.; Novellino, E. Non-nucleoside HIV-1 reverse transcriptase (RT) inhibitors: Past, present, and future perspectives. *Curr. Pharm. Des.* **2002**, *8*, 615–657.
- (6) Schaefer, W.; Friebe, W. G.; Leinert, H.; Mertens, A.; Poll, T.; Von der Saal, W.; Zilch, H.; Nuber, B.; Ziegler, M. L. Non-nucleoside inhibitors of HIV-1 reverse transcriptase: molecular modeling and x-ray structure investigations. *J. Med. Chem.* **1993**, *36*, 726–732.
- (7) Lawtrakul, L.; Beyer, A.; Hannongbua, S.; Wolschann, P. Quantitative Structural Rearrangement of HIV-1 Reverse Transcriptase on Binding to Non-Nucleoside Inhibitors. *Monatsh. Chem.* **2004**, *135*, 1033–1046.
- (8) Das, K.; Clark, A. D., Jr.; Lewi, P. J.; Heeres, J.; De Jonge, M. R.; Koymans, L. M. H.; Vinkers, H. M.; Daeyaert, F.; Ludovici, D. W.; Kukla, M. J.; De Corte, B.; Kavash, R. W.; Ho, C. Y.; Ye, H.; Lichtenstein, M. A.; Andries, K.; Pauwels, R.; De Bethune, M.-P.; Boyer, P. L.; Clark, P.; Hughes, S. H.; Janssen, P. A. J.; Arnold, E. Roles of conformational and positional adaptability in structure-based design of TMC125–R165335 (Etravirine) and related non-nucleoside reverse transcriptase inhibitors that are highly potent and effective against wild-type and drug-resistant HIV-1 variants. *J. Med. Chem.* **2004**, *47*, 2550–2560.
- (9) Hsiou, Y.; Ding, J.; Das, K.; Clark, A. D., Jr.; Boyer, P. L.; Lewi, P.; Janssen, P. A. J.; Kleim, J.-P.; Rosner, M.; Hughes, S. H.; Arnold, E. The Lys103Asn Mutation of HIV-1 RT: A Novel Mechanism of Drug Resistance. *J. Mol. Biol.* **2001**, *309*, 437–445.
- (10) Jacobo-Molina, A.; Ding, J.; Nanni, R. G.; Clark, A. D., Jr.; Lu, X.; Tantillo, C.; Williams, R. L.; Kamer, G.; Ferris, A. L.; et al. Crystal structure of human immunodeficiency virus type 1 reverse transcriptase complexed with double-stranded DNA at 3.0 Å resolution shows bent DNA. *Proc. Natl. Acad. Sci. U.S.A.* **1993**, *90*, 6320–6324.
- (11) Babine, R. E.; Bender, S. L. Molecular Recognition of Protein–Ligand Complexes: Applications to Drug Design. *Chem. Rev.* **1997**, *97*, 1359–1472.
- (12) Greer, J.; Erickson, J. W.; Baldwin, J. J.; Varney, M. D. Application of the three-dimensional structures of protein target molecules in structure-based drug design. *J. Med. Chem.* **1994**, *37*, 1035–1054.
- (13) Kuntz, I. D. Structure-based strategies for drug design and discovery. *Science* **1992**, *257*, 1078–1082.
- (14) Stevens, R. C.; Yokoyama, S.; Wilson, I. A. Global efforts in structural genomics. *Science* **2001**, *294*, 89–92.
- (15) Halperin, I.; Ma, B.; Wolfson, H.; Nussinov, R. Principles of docking: an overview of search algorithms and a guide to scoring functions. *Proteins: Struct. Funct. Genet.* **2002**, *47*, 409–443.
- (16) Waszkowycz, B. New methods for structure-based de novo drug design. *Adv. Drug Discov. Technol.* **1998**, 143–164.
- (17) Verdonk, M. L.; Cole, J. C.; Hartshorn, M. J.; Murray, C. W.; Taylor, R. D. Improved protein–ligand docking using GOLD. *Proteins: Struct. Funct. Genet.* **2003**, *52*, 609–623.
- (18) Eldridge, M. D.; Murray, C. W.; Auton, T. R.; Paolini, G. V.; Mee, R. P. Empirical scoring functions: I. The development of a fast empirical scoring function to estimate the binding affinity of ligands in receptor complexes. *J. Comput.-Aided Mol. Des.* **1997**, *11*, 425–445.

- (19) Kramer, B.; Rarey, M.; Lengauer, T. Evaluation of the FLEXX incremental construction algorithm for protein–ligand docking. *Proteins: Struct. Funct. Genet.* **1999**, *37*, 228–241.
- (20) Claussen, H.; Buning, C.; Rarey, M.; Lengauer, T. FlexE: efficient molecular docking considering Prot. Struc. variations. *J. Mol. Biol.* **2001**, *308*, 377–395.
- (21) Erickson, J. A.; Jalaie, M.; Robertson, D. H.; Lewis, R. A.; Vieth, M. Lessons in Molecular Recognition: The Effects of Ligand and Protein Flexibility on Molecular Docking Accuracy. *J. Med. Chem.* **2004**, *47*, 45–55.
- (22) Goodsell, D. S.; Morris, G. M.; Olson, A. J. Automated docking of flexible ligands: applications of AutoDock. *J. Mol. Recognit.* **1996**, *9*, 1–5.
- (23) Bursulaya, B. D.; Totrov, M.; Abagyan, R.; Brooks, C. L., III Comparative study of several algorithms for flexible ligand docking. *J. Comput.-Aided Mol. Des.* **2004**, *17*, 755–763.
- (24) Titmuss, S. J.; Keller, P. A.; Griffith, R. Docking experiments in the flexible non-nucleoside inhibitor binding pocket of HIV-1 reverse transcriptase. *Bioorg. Med. Chem.* **1999**, *7*, 1163–1170.
- (25) Halgren, T. A.; Murphy, R. B.; Friesner, R. A.; Beard, H. S.; Frye, L. L.; Pollard, W. T.; Banks, J. L. Glide: a new approach for rapid, accurate docking and scoring. 2. Enrichment factors in database screening. *J. Med. Chem.* **2004**, *47*, 1750–1759.
- (26) Zhou, Z.; Madrid, M.; Madura, J. D. Docking of non-nucleoside inhibitors: Neotripterifordin and its derivatives to HIV-1 reverse transcriptase. *Proteins: Struct. Funct. Genet.* **2002**, *49*, 529–542.
- (27) Daeyaert, F.; de Jonge, M.; Heeres, J.; Koymans, L.; Lewi, P.; Vinkers Maarten, H.; Janssen, P. A. J. A pharmacophore docking algorithm and its application to the cross-docking of 18 HIV-NNRTI's in their binding pockets. *Proteins: Struct. Funct. Genet.* **2004**, *54*, 526–533.
- (28) Ranise, A.; Spallarossa, A.; Schenone, S.; Bruno, O.; Bondavalli, F.; Vargiu, L.; Marceddu, T.; Mura, M.; La Colla, P.; Pani, A. Design, Synthesis, SAR, and Molecular Modeling Studies of Acylthiocarbamates: A Novel Series of Potent Non-nucleoside HIV-1 Reverse Transcriptase Inhibitors Structurally Related to Phenylthiazolylthiourea Derivatives. *J. Med. Chem.* **2003**, *46*, 768–781.
- (29) Ragno, R.; Mai, A.; Sbardella, G.; Artico, M.; Massa, S.; Musiu, C.; Mura, M.; Marturana, F.; Cadeddu, A.; La Colla, P. Computer-aided design, synthesis, and anti-HIV-1 activity in vitro of 2-alkylamino-6-[1-(2,6-difluorophenyl)alkyl]-3,4-dihydro-5-alkylpyrimidin-4(3H)-ones as novel potent non-nucleoside reverse transcriptase inhibitors, also active against the Y181C variant. *J. Med. Chem.* **2004**, *47*, 928–934.
- (30) Silvestri, R.; De Martino, G.; Artico, M.; La Regina, G.; Ragno, R.; Loddo, R.; La Colla, P.; Marongiu, M. E.; La Colla, M.; Pani, A. Anti-HIV-1 NNRT agents: acylamino pyrrol aryl sulfones (APASs) as truncated analogues of tricyclic PBTDS. *Med. Chem. Res.* **2002**, *11*, 195–218.
- (31) Di Santo, R.; Costi, R.; Artico, M.; Ragno, R.; Massa, S.; La Colla, M.; Loddo, R.; La Colla, P.; Pani, A. Arylthiopyridylmethylisopropylpyrrole carbinols, novel NNRTIs endowed with potent anti-HIV-1 activity. *Med. Chem. Res.* **2002**, *11*, 153–167.
- (32) Ren, J.; Esnouf, R. M.; Hopkins, A. L.; Jones, E. Y.; Kirby, I.; Keeling, J.; Ross, C. K.; Larder, B. A.; Stuart, D. I.; Stammers, D. K. 3'-Azido-3'-deoxythymidine drug resistance mutations in HIV-1 reverse transcriptase can induce long range conformational changes. *Proc. Natl. Acad. Sci. U.S.A.* **1998**, *95*, 9518–9523.
- (33) Ren, J.; Esnouf, R.; Garman, E.; Somers, D.; Ross, C.; Kirby, I.; Keeling, J.; Darby, G.; Jones, Y.; Stuart, D.; et al. High-resolution structures of HIV-1 RT from four RT-inhibitor complexes. *Nat. Struct. Biol.* **1995**, *2*, 293–302.
- (34) Chan, J. H.; Hong, J. S.; Hunter, R. N. R.; Orr, G. F.; Cowan, J. R.; Sherman, D. B.; Sparks, S. M.; Reitter, B. E.; Andrews, C. W. R.; Hazen, R. J.; St Clair, M.; Boone, L. R.; Ferris, R. G.; Creech, K. L.; Roberts, G. B.; Short, S. A.; Weaver, K.; Ott, R. J.; Ren, J.; Hopkins, A.; Stuart, D. I.; Stammers, D. K. 2-Amino-6-arylsulfonylbenzonitriles as non-nucleoside reverse transcriptase inhibitors of HIV-1. *J. Med. Chem.* **2001**, *44*, 1866–1882.
- (35) Ding, J.; Das, K.; Moereels, H.; Koymans, L.; Andries, K.; Janssen, P. A.; Hughes, S. H.; Arnold, E. Structure of HIV-1 RT/TIBO R 86183 complex reveals similarity in the binding of diverse nonnucleoside inhibitors. *Nat. Struct. Biol.* **1995**, *2*, 407–415.
- (36) Das, K.; Ding, J.; Hsiou, Y.; Clark, A. D. J.; Moereels, H.; Koymans, L.; Andries, K.; Pauwels, R.; Janssen, P. A.; Boyer, P. L.; Clark, P.; Smith, R. H.; Pauwels, R.; Kroeger Smith, M. B.; Michejda, C. J.; Hughes, S. H.; Arnold, E. Crystal structures of 8-Cl and 9-Cl TIBO complexed with wild-type HIV-1 RT and 8-Cl TIBO complexed with the Tyr181Cys HIV-1 RT drug-resistant mutant. *J. Mol. Biol.* **1996**, *264*, 1085–1100.
- (37) Ren, J.; Esnouf, R.; Hopkins, A.; Ross, C.; Jones, Y.; Stammers, D.; Stuart, D. The structure of HIV-1 reverse transcriptase complexed with 9-chloro-TIBO: lessons for inhibitor design. *Structure* **1995**, *3*, 915–926.
- (38) Esnouf, R. M.; Ren, J.; Hopkins, A. L.; Ross, C. K.; Jones, E. Y.; Stammers, D. K.; Stuart, D. I. Unique features in the structure of the complex between HIV-1 reverse transcriptase and the bis-(heteroaryl)piperazine (BHAP) U-90152 explain resistance mutations for this nonnucleoside inhibitor. *Proc. Natl. Acad. Sci. U.S.A.* **1997**, *94*, 3984–3989.
- (39) Ren, J.; Esnouf, R. M.; Hopkins, A. L.; Stuart, D. I.; Stammers, D. K. Crystallographic analysis of the binding modes of thiazoloindolinone non-nucleoside inhibitors to HIV-1 reverse transcriptase and comparison with modeling studies. *J. Med. Chem.* **1999**, *42*, 3845–3851.
- (40) Ding, J.; Das, K.; Tantillo, C.; Zhang, W.; Clark, A. D. J.; Jessen, S.; Lu, X.; Hsiou, Y.; Jacobo-Molina, A.; Andries, K.; et al. Structure of HIV-1 reverse transcriptase in a complex with the nonnucleoside inhibitor alpha-APA R 95845 at 2.8 Å resolution. *Structure* **1995**, *3*, 365–379.
- (41) Pauwels, R.; Andries, K.; Debyser, Z.; Van Daele, P.; Schols, D.; Stoffels, P.; De Vreese, K.; Woestenborghs, R.; Vandamme, A. M.; Janssen, C. G.; et al. Potent and highly selective human immunodeficiency virus type 1 (HIV-1) inhibition by a series of alpha-anilinothiophenylacetamide derivatives targeted at HIV-1 reverse transcriptase. *Proc. Natl. Acad. Sci. U.S.A.* **1993**, *90*, 1711–1715.
- (42) Ren, J.; Milton, J.; Weaver, K. L.; Short, S. A.; Stuart, D. I.; Stammers, D. K. Structural basis for the resilience of efavirenz (DMP-266) to drug resistance mutations in HIV-1 reverse transcriptase. *Struct. Fold. Des.* **2000**, *8*, 1089–1094.
- (43) Corbett, J. W.; Ko, S. S.; Rodgers, J. D.; Jeffrey, S.; Bachelier, L. T.; Klabe, R. M.; Diamond, S.; Lai, C. M.; Rabel, S. R.; Saye, J. A.; Adams, S. P.; Trainor, G. L.; Anderson, P. S.; Erickson-Viitanen, S. K. Expanded-spectrum nonnucleoside reverse transcriptase inhibitors inhibit clinically relevant mutant variants of human immunodeficiency virus type 1. *Antimicrob. Agents Chemother.* **1999**, *43*, 2893–2897.
- (44) Lindberg, J.; Sigurdsson, S.; Lowgren, S.; Andersson, H. O.; Sahlberg, C.; Noreen, R.; Fridborg, K.; Zhang, H.; Unge, T. Structural basis for the inhibitory efficacy of efavirenz (DMP-266), MSC194 and PNU142721 towards the HIV-1 RT K103N mutant. *Eur. J. Biochem.* **2002**, *269*, 1670–1677.
- (45) Ren, J.; Nichols, C.; Bird, L.; Chamberlain, P.; Weaver, K.; Short, S.; Stuart, D. I.; Stammers, D. K. Structural mechanisms of drug resistance for mutations at codons 181 and 188 in HIV-1 reverse transcriptase and the improved resilience of second generation non-nucleoside inhibitors. *J. Mol. Biol.* **2001**, *312*, 795–805.
- (46) Hopkins, A. L.; Ren, J.; Tanaka, H.; Baba, M.; Okamoto, M.; Stuart, D. I.; Stammers, D. K. Design of MKC-442 (emivirine) analogues with improved activity against drug-resistant HIV mutants. *J. Med. Chem.* **1999**, *42*, 4500–4505.
- (47) Hsiou, Y.; Das, K.; Ding, J.; Clark, A. D. J.; Kleim, J. P.; Rosner, M.; Winkler, I.; Riess, G.; Hughes, S. H.; Arnold, E. Structures of Tyr188Leu mutant and wild-type HIV-1 reverse transcriptase complexed with the non-nucleoside inhibitor HBV 097: inhibitor flexibility is a useful design feature for reducing drug resistance. *J. Mol. Biol.* **1998**, *284*, 313–323.
- (48) Hopkins, A. L.; Ren, J.; Esnouf, R. M.; Willcox, B. E.; Jones, E. Y.; Ross, C.; Miyasaka, T.; Walker, R. T.; Tanaka, H.; Stammers, D. K.; Stuart, D. I. Complexes of HIV-1 reverse transcriptase with inhibitors of the HEPT series reveal conformational changes relevant to the design of potent non-nucleoside inhibitors. *J. Med. Chem.* **1996**, *39*, 1589–1600.
- (49) Hogberg, M.; Sahlberg, C.; Engelhardt, P.; Noreen, R.; Kangas-metsa, J.; Johansson, N. G.; Oberg, B.; Vrang, L.; Zhang, H.; BL, S.; Unge, T.; Lovgren, S.; Fridborg, K.; Backbro, K. Urea-PETT compounds as a new class of HIV-1 reverse transcriptase inhibitors. 3. Synthesis and further structure–activity relationship studies of PETT analogues. *J. Med. Chem.* **1999**, *42*, 4150–4160.
- (50) Ren, J.; Diprose, J.; Warren, J.; Esnouf, R. M.; Bird, L. E.; Ikemizu, S.; Slater, M.; Milton, J.; Balzarini, J.; Stuart, D. I.; Stammers, D. K. Phenylethylthiazolylthiourea (PETT) non-nucleoside inhibitors of HIV-1 and HIV-2 reverse transcriptases. Structural and biochemical analyses. *J. Biol. Chem.* **2000**, *275*, 5633–5639.
- (51) Ren, J.; Nichols, C.; Bird, L. E.; Fujiwara, T.; Sugimoto, H.; Stuart, D. I.; Stammers, D. K. Binding of the second generation non-nucleoside inhibitor S-1153 to HIV-1 reverse transcriptase involves extensive main chain hydrogen bonding. *J. Biol. Chem.* **2000**, *275*, 14316–14320.
- (52) Ren, J.; Esnouf, R. M.; Hopkins, A. L.; Warren, J.; Balzarini, J.; Stuart, D. I.; Stammers, D. K. Crystal structures of HIV-1 reverse transcriptase in complex with carboxanilide derivatives. *Biochemistry* **1998**, *37*, 14394–14403.

- (53) Wang, J.; Morin, P.; Wang, W.; Kollman, P. A. Use of MM-PBSA in reproducing the binding free energies to HIV-1 RT of TIBO derivatives and predicting the binding mode to HIV-1 RT of efavirenz by docking and MM-PBSA. *J. Am. Chem. Soc.* **2001**, *123*, 5221–5230.
- (54) Rao, G. S.; Bhatnagar, S. In silico structure-based design of a potent, mutation resilient, small peptide inhibitor of HIV-1 reverse transcriptase. *J. Biomol. Struct. Dyn.* **2003**, *21*, 171–178.
- (55) Ragno, R.; Mai, A.; Massa, S.; Cerbara, I.; Valente, S.; Bottoni, P.; Scatena, R.; Jesacher, F.; Loidl, P.; Brosch, G. 3-(4-Aroyl-1-methyl-1H-pyrrol-2-yl)-N-hydroxy-2-propenamides as a New Class of Synthetic Histone Deacetylase Inhibitors. 3. Discovery of Novel Lead Compounds through Structure-Based Drug Design and Docking Studies. *J. Med. Chem.* **2004**, *47*, 1351–1359.
- (56) Hsiou, Y.; Ding, J.; Das, K.; Clark, A. D., Jr.; Hughes, S. H.; Arnold, E. Structure of unliganded HIV-1 reverse transcriptase at 2.7 Å resolution: implications of conformational changes for polymerization and inhibition mechanisms. *Structure* **1996**, *4*, 853–860.
- (57) Jager, J.; Smerdon, S. J.; Wang, J.; Boisvert, D. C.; Steitz, T. A. Comparison of three different crystal forms shows HIV-1 reverse transcriptase displays an internal swivel motion. *Structure* **1994**, *2*, 869–876.
- (58) Patel, P. H.; Jacobo-Molina, A.; Ding, J.; Tantillo, C.; Clark, A. D., Jr.; Raag, R.; Nanni, R. G.; Hughes, S. H.; Arnold, E. Insights into DNA polymerization mechanisms from structure and function analysis of HIV-1 reverse transcriptase. *Biochemistry* **1995**, *34*, 5351–5363.
- (59) Kroeger Smith, M. B.; Rouzer, C. A.; Taneyhill, L. A.; Smith, N. A.; Hughes, S. H.; Boyer, P. L.; Janssen, P. A.; Moereels, H.; Koymans, L.; Arnold, E.; et al. Molecular modeling studies of HIV-1 reverse transcriptase nonnucleoside inhibitors: total energy of complexation as a predictor of drug placement and activity. *Protein Sci.* **1995**, *4*, 2203–2222.
- (60) Birch, L.; Murray, C. W.; Hartshorn, M. J.; Tickle, I. J.; Verdonk, M. L. Sensitivity of molecular docking to induced fit effects in influenza virus neuraminidase. *J. Comput.-Aided Mol. Des.* **2003**, *16*, 855–869.
- (61) Carlson, H. A.; McCammon, J. A. Accommodating protein flexibility in computational drug design. *Mol. Pharm.* **2000**, *57*, 213–218.
- (62) Osterberg, F.; Morris, G. M.; Sanner, M. F.; Olson, A. J.; Goodsell, D. S. Automated docking to multiple target structures: incorporation of protein mobility and structural water heterogeneity in Autodock. *Proteins: Struct. Funct. Genet.* **2001**, *46*, 34–40.
- (63) Vieth, M.; Hirst, J. D.; Kolinski, A.; Brooks, C. L., III Assessing energy functions for flexible docking. *J. Comput. Chem.* **1998**, *19*, 1612–1622.
- (64) Ragno, R.; Artico, M.; De Martino, G.; La Regina, G.; Coluccia, A.; Di Pasquali, A.; Silvestri, R. Docking and 3-D QSAR Studies on Indolyl Aryl Sulfones (IASs). Binding Mode Exploration at the HIV-1 Reverse Transcriptase Non-Nucleoside Binding Site and Design of Highly Active N-(2-Hydroxyethyl)carboxamide and N-(2-Hydroxyethyl)carboxy hydrazide Derivatives. *J. Med. Chem.*, in press.
- (65) Silvestri, R.; De Le Martino, G.; La Regina, G.; Artico, M.; Massa, S.; Vargiu, L.; Mura, M.; Loi, A. G.; Marceddu, T.; La Colla, P. Novel Indolyl Aryl Sulfones Active against HIV-1 Carrying NNRTI Resistance Mutations: Synthesis and SAR Studies. *J. Med. Chem.* **2003**, *46*, 2482–2493.
- (66) Berman, H.; Henrick, K.; Nakamura, H. Announcing the worldwide Protein Data Bank. *Nat. Struct. Biol.* **2003**, *10*, 980.
- (67) Berman, H. M.; Westbrook, J.; Zarddecki, C.; Bourne, P. E. The protein data bank. *Prot. Struct.* **2003**, 389–405.
- (68) Berman, H. M.; Westbrook, J.; Feng, Z.; Gilliland, G.; Bhat, T. N.; Weissig, H.; Shindyalov, I. N.; Bourne, P. E. The Protein Data Bank. *Nucleic Acids Res.* **2000**, *28*, 235–242.
- (69) Martin, A. C. R. *Profit 2.2*; <http://www.bioinf.org.uk/software/profit/>.
- (70) McLachlan, A. D. Rapid comparison of Prot. Struct. *Acta Crystallogr., Sect. A: Fundam. Crystallogr.* **1982**, *A38*, 871–873.
- (71) Huang, C. C.; Couch, G. S.; Pettersen, E. F.; Ferrin, T. E. In *Chimera: An Extensible Molecular Modeling Application Constructed Using Standard Components*; Pacific Symposium on Biocomputing: **1996**, *1*, 724.
- (72) *Maestro 3.1*; Schrodinger, Inc.: Portland, OR, 2001.
- (73) Mohamadi, F.; Richards, N. G. J.; Guida, W. C.; Liskamp, R.; Lipton, M.; Caufield, C.; Chang, G.; Hendrickson, T.; Still, W. C. MacroModel-An Integrated Software System for Modeling Organic and Bioorganic Molecules Using Molecular Mechanics. *J. Comput. Chem.* **1990**, *11*, 440–467.
- (74) Pearlman, D. A.; Case, D. A.; Caldwell, J. W.; Ross, W. S.; Cheatham, T. E., III; DeBolt, S.; Ferguson, D.; Seibel, G.; Kollman, P. “AMBER”, a package of computer programs for applying molecular mechanics, normal mode analysis, molecular dynamics and free energy calculations to simulate the structural and energetic properties of molecules. *Comput. Phys. Comm.* **1995**, *91*, 1–42.
- (75) Sotriffer, C. A.; Ni, H. H.; McCammon, J. A. Binding modes of HIV-1 integrase inhibitors at the active site. *Rational Approaches to Drug Design, Proceedings of the European Symposium on Quantitative Structure–Activity Relationships*, 13th, Duesseldorf, Germany, Aug 27 to Sept 1, 2000; Prous Science: Barcelona, Spain, 2001; pp 83–87.

JM0493921